SCIENCE CHINA
Life Sciences

July 2010 Vol.53 No.7: 784–797
doi: 10.1007/s11427-010-4025-1

Changes in the distribution of South Korean forest vegetation simulated using thermal gradient indices

CHOI Sungho[1], LEE Woo-Kyun[1*], SON Yowhan[1], YOO Seongjin[1] & LIM Jong-Hwan[2]

[1] *Department of Environmental Science and Ecological Engineering, Korea University, Seoul 136-713, Korea;*
[2] *Korea Forest Research Institute, Seoul 130-712, Korea*

Received February 9, 2010; accepted April 3, 2010

To predict changes in South Korean vegetation distribution, the Warmth Index (WI) and the Minimum Temperature of the Coldest Month Index (MTCI) were used. Historical climate data of the past 30 years, from 1971 to 2000, was obtained from the Korea Meteorological Administration. The Fifth-Generation National Center for Atmospheric Research (NCAR) /Penn State Mesoscale Model (MM5) was used as a source for future climatic data under the A1B scenario from the Special Report on Emission Scenario (SRES) of the Intergovernmental Panel on Climate Change (IPCC). To simulate future vegetation distribution due to climate change, the optimal habitat ranges of Korean tree species were delimited by the thermal gradient indices, such as WI and MTCI. To categorize the Thermal Analogy Groups (TAGs) for the tree species, the WI and MTCI were orthogonally plotted on a two-dimensional grid map. The TAGs were then designated by the analogue composition of tree species belonging to the optimal WI and MTCI ranges. As a result of the clustering process, 22 TAGs were generated to explain the forest vegetation distribution in Korea. The primary change in distribution for these TAGs will likely be in the shrinkage of areas for the TAGs related to *Pinus densiflora* and *P. koraiensis,* and in the expansion of the other TAG areas, mainly occupied by evergreen broad-leaved trees, such as *Camellia japonica*, *Cyclobalanopsis glauca*, and *Schima superba.* Using the TAGs to explain the effects of climate change on vegetation distribution on a more regional scale resulted in greater detail than previously used global or continental scale vegetation models.

climate change, forest distribution, warmth index, minimum temperature, thermal analogy group

Citation: Choi S, Lee W K, Son Y, *et al*. Changes in the distribution of South Korean forest vegetation simulated using thermal gradient indices. Sci China Life Sci, 2010, 53: 784−797, doi: 10.1007/s11427-010-4025-1

According to the assessment of annual average temperatures by the Intergovernmental Panel on Climate Change (IPCC), a global temperature increase of 0.74°C has occurred over the past 100 years. This may further increase by another 1.1–6.4°C by the 2090s [1]. The recent effect of global warming related climate change on forest ecosystems is a major focus for the IPCC [2]. Forest vegetation plays an important role in climatic processes, especially in its contribution to heat and moisture fluxes. Conversely, changes in climate can also result in changes in forest distribution. Therefore, assessment of changes in forest vegetation distribution, and the relationship of such to climate change, is a requirement for better understanding of climatic processes [3–8].

There have been many previous studies using vegetation models to understand the effects of climate change on the distribution of ecosystems [9–11]. These Dynamic Global Vegetation Models (DGVMs) have helped explain historical changes in carbon and in vegetation distribution and have provided a basis for future prediction of such changes based on climatic scenarios [12–15]. For example, the MAPSS-

*Corresponding author (email: leewk@korea.ac.kr)

CENTURY (MC1) model, designed by the United States Department of Agriculture (USDA), was applied in California to evaluate the effects of climate change on vegetation distribution and ecosystem productivity [16,17]. In China, model simulations for Carbon Exchange between Vegetation, Soil, and Atmosphere (CEVSA), have predicted that as a result of climate change, mixed forest and deciduous broad-leaved forest are likely to expand northward, and that shrubland and grassland will become widespread in south China [18].

There have also been many trials applying previous DGVMs to evaluate the impact of climate change on Korean ecosystems. However, no national vegetation models have been developed in Korea. Kim *et al*. [19] suggested that simulations of previous DGVMs, such as Holdridge [20], CEVSA [21] and MC1 [22], have provided useful estimates of the vulnerability of Korean forest ecosystems by using historical climatic data combined with future predictive modeling. However, these models, mostly designed and tested for global or continental scale assessment, were unable to provide accurate results for Korea on a regional scale [19,21,22]. In the MC1 models for estimating the potential vegetation distribution in Korea, only four [23] Plant Functional Types (PFTs) were specified to attempt to summarize vegetation distribution over the whole of South Korea. The tree classification thresholds of these models were, therefore, relatively coarse for simulating the Korean territory [23]. A similar situation has arisen in European analysis due to the spatial heterogeneity of European ecosystems, where the limited number of PFTs used for DGVMs resulted in a lack of accuracy on a regional scale [7]. According to Riera *et al*. [24], the spatial heterogeneity of vegetation is influenced by microenvironments, competition processes, or disturbances on a small or medium (regional) scale. In contrast, large-scale (global) models usually employ calculations of mean vegetation distribution as constrained by global climate and elevation. Therefore, it is necessary to adopt different approaches for modeling on a regional, as opposed to a global, scale. Our goal is to simulate and predict Korean vegetation distribution on a smaller and more detailed regional scale using climatic variables; this is in contrast to previous studies, which have had a more global application.

Biomes are most basically defined as areas of vegetation containing the same life forms. Their distributions are usually correlated to climatic conditions [25–27]. Underlying physiological processes have been discovered and used to explain how plants respond to environmental stress [28–30]. As stated by Arris and Eagleson [3] and Wang *et al*. [31], temperature is known to be one of the most important variables influencing the patterns of vegetation distribution. Temperature also affects vegetation metabolism and the growth of woody plants [32]. Tree species vary widely in their optimal growth temperatures and/or in their tolerance to sub-zero conditions [33,34].

In previous studies, patterns of potential forest cover were predicted along thermal gradient indices, such as Kira's Warmth Index (WI) [35–40] and the Minimum Temperature of the Coldest month (MTC) [5,6,8]. The WI has long been recognized as an important index for predicting potential vegetation distribution. However, recently, extreme cold, measured as the minimum winter temperature, has been suggested as the principal factor determining the northern limit of the natural range of the Japanese beech (*Fagus crenata)* in Japan [5,6] and of Sub-arctic Conifers [34]. The key aspect was the relationship between cold and injury or death of extra organs, such as twigs. Strimbec *et al*. [41] also mentioned that an understanding of the mechanisms of low temperature tolerance and the degree to which they are employed in various plant taxa, are important in predicting the effects of climate change on tree and forest health and productivity. Therefore, the Japanese studies used both the WI and MTC to predict climate change effects upon *Fagus crenata* distribution [5,6]. In contrast, using the MTC to predict the spatial limits of forest vegetation has not yet been attempted in a Korean context even though the use of WI had shown a reasonable spatial distribution of forest vegetation for four vegetation groups: subalpine, cool-temperate, warm-temperate deciduous and warm-temperate evergreen [35,36,40].

The full application of both the WI and MTC is therefore required to explain the forest vegetation distribution and assess and predict the effects of climate change on forest cover throughout Korea. The objectives of this study are to simulate the potential distribution of forest vegetation in Korea using the optimal habitat ranges provided by both the WI and the MTC Index (MTCI) and then to predict the changes in spatial distribution of forest cover due to climate change using both of these indices.

1 Materials and methods

1.1 Study area and meteorological data preparation

The whole of South Korea, longitude 124°54′–131°06′ and latitude 33°09′–38°45′, was under study and was presented as raster data with 0.01° spatial resolution. A key feature is the Taebaek Mountain Range, running along the eastern edge of the Korean peninsula, rising to over 1500 m. Another range, the Sobaek Mountain Range, splits off from the Taebaek Mountains in the northeast heading southwest across the center of the peninsula. In the central zone, moderately high mountains dominate. Lowlands are found mainly along the western regions (Figure 1A) [42]. According to 2008 data, evergreen needle-leaved forests (mainly *Pinus densiflora*–55.0%) and deciduous broad-leaved forests (mainly *Quercus* spp.) occupy approximately 42% (2860000 ha) and 26% (1659000 ha) of South Korea's total forest areas, respectively [43] (Figure 1B). These two

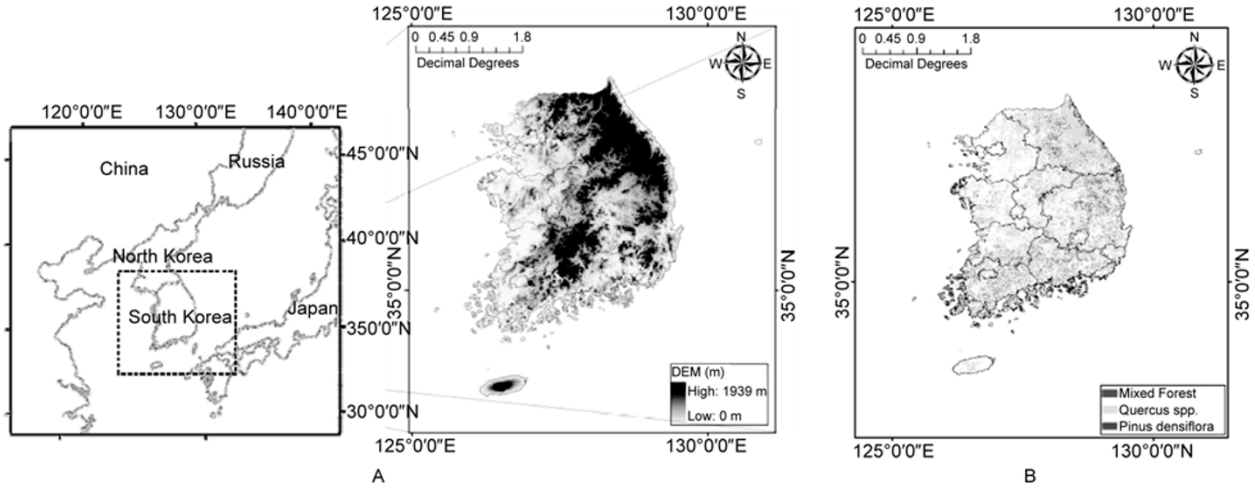

Figure 1 Digital Elevation Model of Korea (A) and the Actual forest types in Korea (B).

species are of considerable importance in Korea for their ecological, economic and socio-cultural values [44].

Climatic data sets were prepared for three periods: (i) historic (1971–2000), (ii) near future (2021–2050), and (iii) far future (2071–2100). The Korea Meteorological Administration (KMA) provided the historical climate data, including that of monthly mean temperatures and mean daily minimum temperatures. These were obtained from 75 weather stations distributed throughout South Korea and covered the period from 1971 to 2000. These data sets were interpolated with a 0.01° grid size using Inverse Distance Squared Weighting (IDSW), a spatial statistical method, with respect to the absolute temperature lapse rate by altitude [45]. In addition, future climate data was predicted using the Fifth-Generation National Center for Atmospheric Research (NCAR)/Penn State Mesoscale Model (MM5) coupled with ECHO-G under the A1B scenario (Special Report on Emission Scenario of IPCC) by the National Institute of Meteorological Research (NIMR) with a 0.2432° grid size [46,47]. These datasets were then resampled to a 0.01° spatial resolution in the WGS-84 coordinate system [45].

1.2 Calculation of thermal indices: WI and MTCI

The Warmth Index (WI) of Kira [48] was prepared for each pixel using equation 1 which counts the annual sum of positive differences between monthly means and 5°C.

$$WI = \sum (t - 5), \tag{1}$$

where t is the monthly mean temperature above 5°C.

The second thermal index employed was the Minimum Temperature of the Coldest Month Index (MTCI). According to Bachelet *et al*. [12], needle-leaved tree species appear when the Minimum Temperature of the Coldest Month (MTC) drops below −15°C. When the MTC is above 18°C, broad-leaved evergreen species are predicted to appear. Theoretically, evergreen needle-leaved species can dominate below a MTC of −15°C, deciduous broad-leaved species are likely to appear around an MTC of 1.5°C, and evergreen broad-leaved species appear above an MTC of 18°C. This follows the logic of Neilson [49] in identifying the leaf longevity and shape of vegetation species. To stretch the range of MTC and classify vegetation species more widely, Bachelet *et al*. [12] suggested two equations to produce the MTCI. The MTC was converted using equations 2 and 3. Both the WI and MTCI are important thermal indices because they are correlated to the effective optimal habitat temperature for plants and the freeze resistance of tree species, respectively [48,49]. Matsui *et al*. [5,6] mentioned that the WI and MTC were important indices to evaluate the relationships of climatic factors to the presence/absence of *Fagus crenata* in their tree classification model.

$$MTCI = \frac{MTC - t_{\text{mid}}}{t_{\text{hi}} - t_{\text{mid}}} \times 100 \quad MTC \geqslant t_{\text{mid}}\ (1.5°\text{C}), \tag{2}$$

$$MTCI = \frac{t_{\text{mid}} - MTC}{t_{\text{mid}} - t_{\text{low}}} \times (-100) \quad MTC < t_{\text{mid}}\ (1.5°\text{C}), \tag{3}$$

where t_{hi}, t_{mid}, and t_{low} are 18, 1.5, and −15°C, respectively.

1.3 Integration of WI and MTCI

The Empirical Orthogonal Function (EOF) has been used in many research fields, such as atmospheric science and oceanography, to recognize spatial and temporal patterns among environmental variables [50]. It is a useful method for simplifying large data sets and diagnosing dominant patterns of variables in geophysical data sets. This method helps in delineating areas that have similar climatic variability [51–53]. For example, Timmermann [54] implemented the two dominant EOFs of annually averaged sur-

face temperature to show the typical El Nino structure with its characteristic strong warming in both the eastern equatorial Pacific and the Tropics. Yim [36] also used the WI and Coldness Index (CI) to ordinate forest types by orthogonal integration. In this study, an EOF analysis was carried out to delineate the spatial distribution of the WI and MTCI in Korea. The horizontal variable of EOF corresponds to WI and the vertical variable of EOF relates to MTCI. This orthogonal integration of the WI and MTCI was applied to classify areas with similar climatic thermal indices.

1.4 Clustering the Thermal Analogy Groups (TAGs) using optimal WI and MTCI ranges

The optimal WI ranges of a number of tree species were calculated by Yim [35,36]. These included five evergreen needle-leaved trees, eight deciduous broad-leaved trees, and one evergreen broad-leaved tree, all of which had been previously validated by Yang and Shim [40]. Additionally the optimal ranges of two evergreen needle-leaved trees, one deciduous broad-leaved, and three evergreen broad-leaved trees were obtained from Fang and Yoda [37–39] because the tree species used by Yim [35,36] were not sufficient to explain the WI ranges over 125°C a month in Korea.

Regarding the MTCI, there have been insufficient studies on the optimal ranges of this index for each species as compared with those related to the WI. Thus, this study suggested a linear stretch method of Minimum-Maximum Contrast Stretch, utilizing remote sensing techniques, to identify MTCI ranges using the WI ranges (equation 4) [55]. This method is usually applied to expand the original values into a new distribution by considering the maximum and minimum ranges of the original values [55]. The optimal WI and the converted optimal MTCI ranges for each species are listed in Table 1. Matsui *et al*. [5] mentioned that their classification tree model resulted in the highest possibility of *F. crenata* occurrence in the WI range of 77.15–85.15°C·month and MTC of −12.25– −3.25°C (equal to −83.33– −28.79 of MTCI). As a result of converting the WI range for *F. crenata* using equation 4, the MTCI for *F. crenata* ranged from −76.4 to −63.4, thus occurring within the MTCI range of Matsui *et al*. [5]. Therefore, this equation, which applies the WI ranges, was suggested to be adequate for assigning the optimal MTCI range for each tree species.

$$MTCI = \left(\frac{MTCI_{\max} - MTCI_{\min}}{WI_{\max} - WI_{\min}} \right) \times \left(WI - WI_{\min} \right) + MTCI_{\min}. \quad (4)$$

For clustering of South Korean tree species, the WI and MTCI were plotted on a two-dimensional grid map (EOF map). Grid cells according to the WI and MTCI of past years (1971–2000) are shown in gray (area *A in Figure 2). Tree species codes were assigned in each grid cell corresponding to their optimal WI and MTCI ranges. Each pixel was delimited by both the optimal WI and MTCI relating to the high possibility of tree species occurrence. The Thermal Analogy Groups (TAGs) were then designated by the analogue composition of tree species in each grid cell. For in-

Table 1 Optimal WI and MTCI ranges for each species

***Species code	Tree species	Optimal WI range (°C·month)	Optimal MTCI range
A1	*Abies nephrolepis*	*34.0–65.0	−146.4– −96.1
A2	*Taxus cuspidata*	*37.0–62.0	−141.5– −101.0
A3	*Pinus koraiensis*	*45.0–81.0	−128.5– −70.2
A4	*P. densiflora*	*60.0–95.0	−104.2– −47.5
A5	*P. thunbergii*	*93.0–104.0	−50.7– −32.9
A6	*P. massoniana*	**112.3–159.5	−19.4–57.4
A7	*P. yunnanensis*	**90.5–147.1	−54.7–37.0
B1	*Quercus mongolica*	*46.0–90.0	−126.9– −55.6
B2	*Carpinus laxiflora*	*67.0–94.0	−92.9– −49.1
B3	*Q. dentata*	*75.0–97.0	−79.9– −44.2
B4	*C. tschonoskii*	*77 .0–103.0	−76.7– −34.5
B5	*Q. serrata*	*67.0–92.0	−92.9– −52.3
B6	*Q. aliena*	*75.0–91.0	−79.9– −54
B7	*Q. variabilis*	*77.0–95.0	−76.7– −47.5
B8	*Q. acutissima*	*85.0–99.0	−63.7– −47.5
B9	*Fagus lucida*	**87.3–120.9	−60.0– −5.5
C1	*Camellia japonica*	*100.0–125.0	−39.4–1.2
C2	*Cyclobalanopsis glauca*	**97.6–137.4	−43.3–21.3
C3	*Schima superba*	**112.4–153.0	−19.2–46.7
C4	*Castanopsis indica*	**138.1–178.4	22.4–87.8

*, From Yim [35,36]. **, From Fang and Yoda [37–39]. ***, Species code A: evergreen needle-leaved trees; code B: deciduous broad-leaved trees; and code C: evergreen broad-leaved trees.

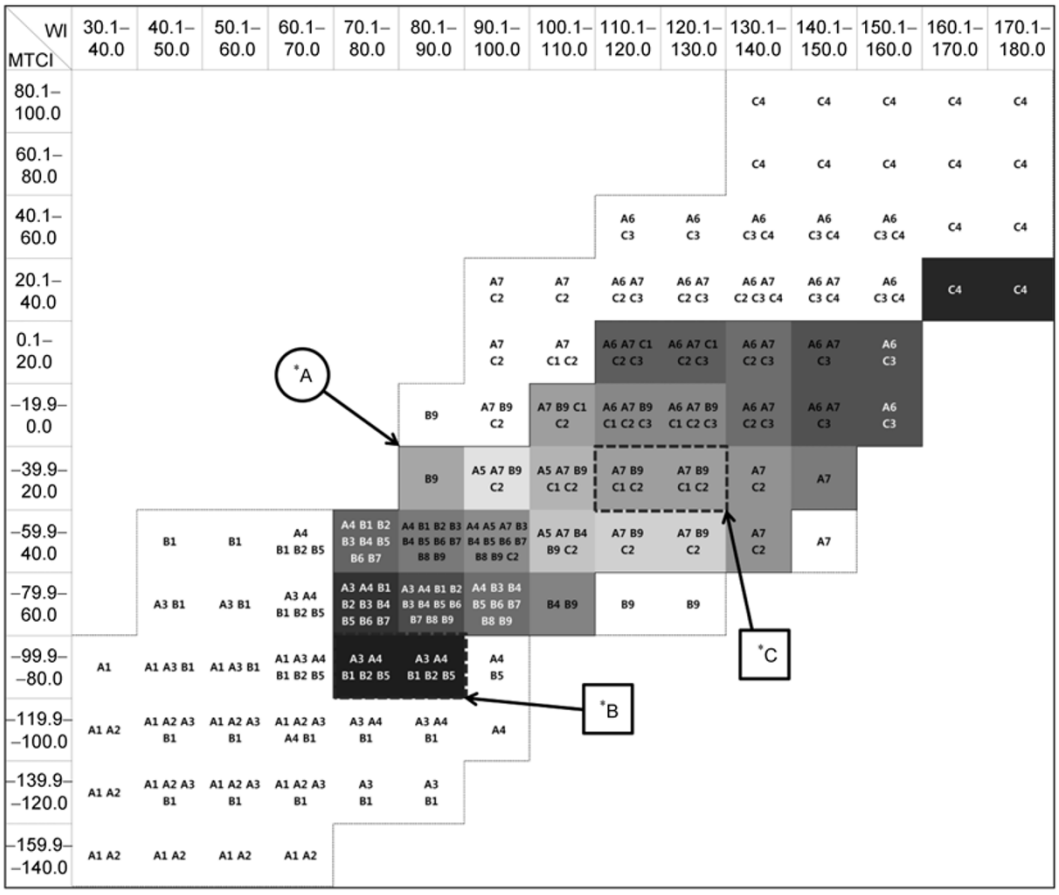

Figure 2 Assigned tree species codes by the optimal WI and MTCI ranges. *A, Grid cells of the integration of WI and MTCI of past years (1971–2000) within Korean territory in differing shades of gray. Two example of TAGs: (1) dashed rectangle *B and (2) dashed rectangle *C.

stance, the grid cells composed of tree species codes A3, A4, B1, B2, and B5 (in dashed rectangle, *B in Figure 2) were grouped as one TAG. In addition, the composition of the tree species codes A7, B9, C1, and C2 (in dotted rectangle, *C in Figure 2) determine the other TAGs. These classified TAGs can depict the potential forest cover distribution for past and future because each TAG is highly related to the optimal habitats for those tree species.

1.5 Model verification

The results of TAG simulation were verified by classification accuracy (CA). Matsui *et al*. [5] employed the CA equation 5 from Iverson and Prasad [56] to assess their predictions of forest distribution.

$$CA = \frac{A_{\text{both}}}{A_{\text{act}} + TA_{\text{pred}}} \times 100, \quad (5)$$

where A_{both} is the area identified with focal species present in both the 4th forest type map of the Korea Forest Service (KFS) and the simulated results. A_{act} is the area identified only in the forest type map of KFS and TA_{pred} is the area identified in the simulated results.

If the CA values are close to 100 percent, it means that the result of predicted distribution is likely to be accurately simulating the past and future vegetation distribution. As in the study of Matsui *et al*. [5], anthropogenically affected areas were excluded during the verification process because they were not considered in the TAG simulation.

2 Results and discussion

2.1 WI and MTCI distribution in Korea

Yim [35,36] and Fang and Yoda [37–39], using the WI and forming a thermal distribution curve for each species, suggested both the potential whole range and optimal habitat range for several tree species. Yim [35,26] grouped tree species into four groups according to their thermal distribution ranges in Korea: subalpine, cool-temperate, warm-temperate deciduous and warm-temperate evergreen. In addition, Fang and Yoda [37–39] classified seven range groups in China: subarctic conifers, sub-arctic-cool-temperate transient, cool-temperate, cool-temperate-warm-temperate transient, warm-temperate, southern warm-temperate, and subtropical/tropical.

Historically, (1971–2000), the WI for Korea has ranged from 71.28 to 132.81°C·month (Table 2). This corresponds to the criteria of Yim [35] for cool-temperate species (range: 50–90°C·month), warm-temperate deciduous (range: 80–100°C·month) and evergreen species (range: 100–120°C·month). This WI distribution characteristic was likely to be related to the latitudinal and altitudinal patterns correlated to dominant tree species of forest ecosystems [4,57]. However, predictions for Korea, suggest there will be an overall WI increase in the near future, ranging from 81.18 to 147.73 (2021–2050) continuing in the far future, from 97.54 to 174.19°C·month (2071–2100). The upper limits of such a future WI predictions are outside the ranges of the aforementioned categories. However, such a range was covered by vegetation zones included in Fang and Yoda [39], such as a warm-temperate evergreen broadleaf forest (range: 90–175°C·month), and the southern warm-temperate subzone (range: 135–175°C·month). This vegetation zoning procedure, based on the WI alone, remains too broad and is therefore inadequate for explaining the more detailed vegetation distribution situation in Korea for either historical or future predictive modeling.

To solve this issue, the incorporation of MTCI may help more precisely categorize regional forest distribution as a supplementary index for the WI. The MTCI distribution of Korea in past years ranged from −84.97 to 14.36 (Table 2). For predicting effects of climate change, the MTCI has a wider-scope of values and narrower fluctuations at the upper limits of values than does the WI. The MTCI is predicted to decline in the future, ranging from −80.91 to 19.82 (2021–2050) and from −58.79 to 34.73 (2071–2100).

Table 2 WI and MTCI ranges in Korea

Time period	WI range (°C·month)	MTCI range
Past (1971–2000)	71.28–132.81	−84.97–14.36
Near future (2021–2050)	81.18–147.73	−80.91–19.82
Far future (2071–2100)	97.54–174.19	−58.79–34.73

Regarding the spatial distribution of the WI and MTCI in Korea, their past distribution patterns are clearly linked to topographic features (Figures 3A and 4A) being lower in the northeast and higher in the southwest, in a manner directly corresponding to altitude (Figure 1A). Future effects of climate change on the spatial distribution of the WI and MTCI are depicted in Figures 3B, 3C, 4B and 4C. Generally,

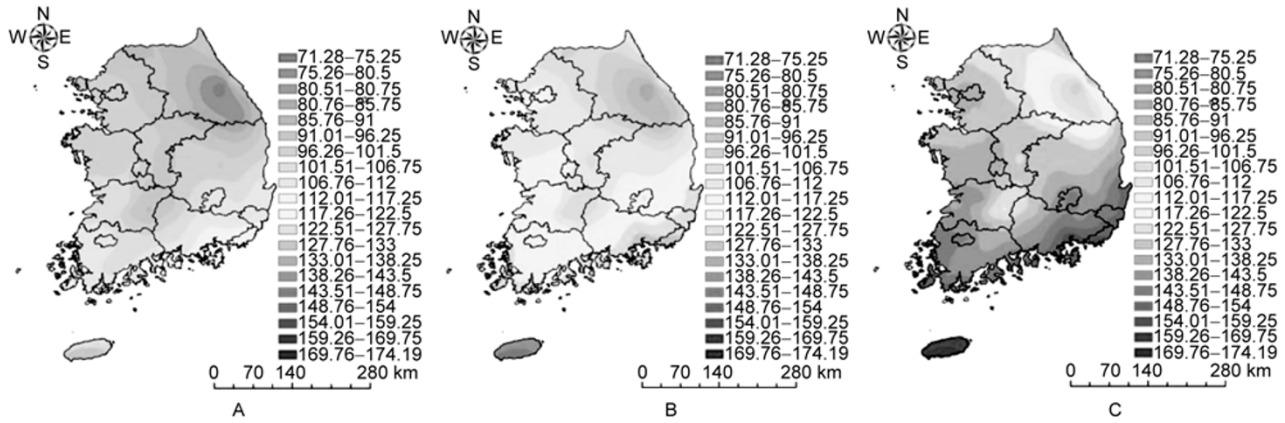

Figure 3 WI distributions of the past (1971–2000) (A), near future (2021–2050) (B), and far future (2071–2100) in Korea (C).

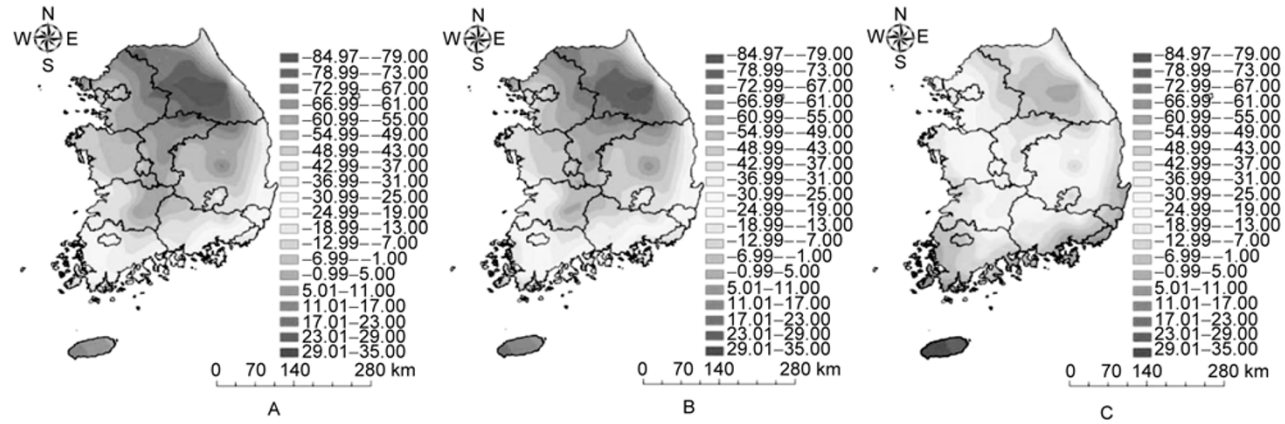

Figure 4 MTCI distributions of the past (1971–2000) (A), near future (2021–2050) (B), and far future (2071–2100) in Korea (C).

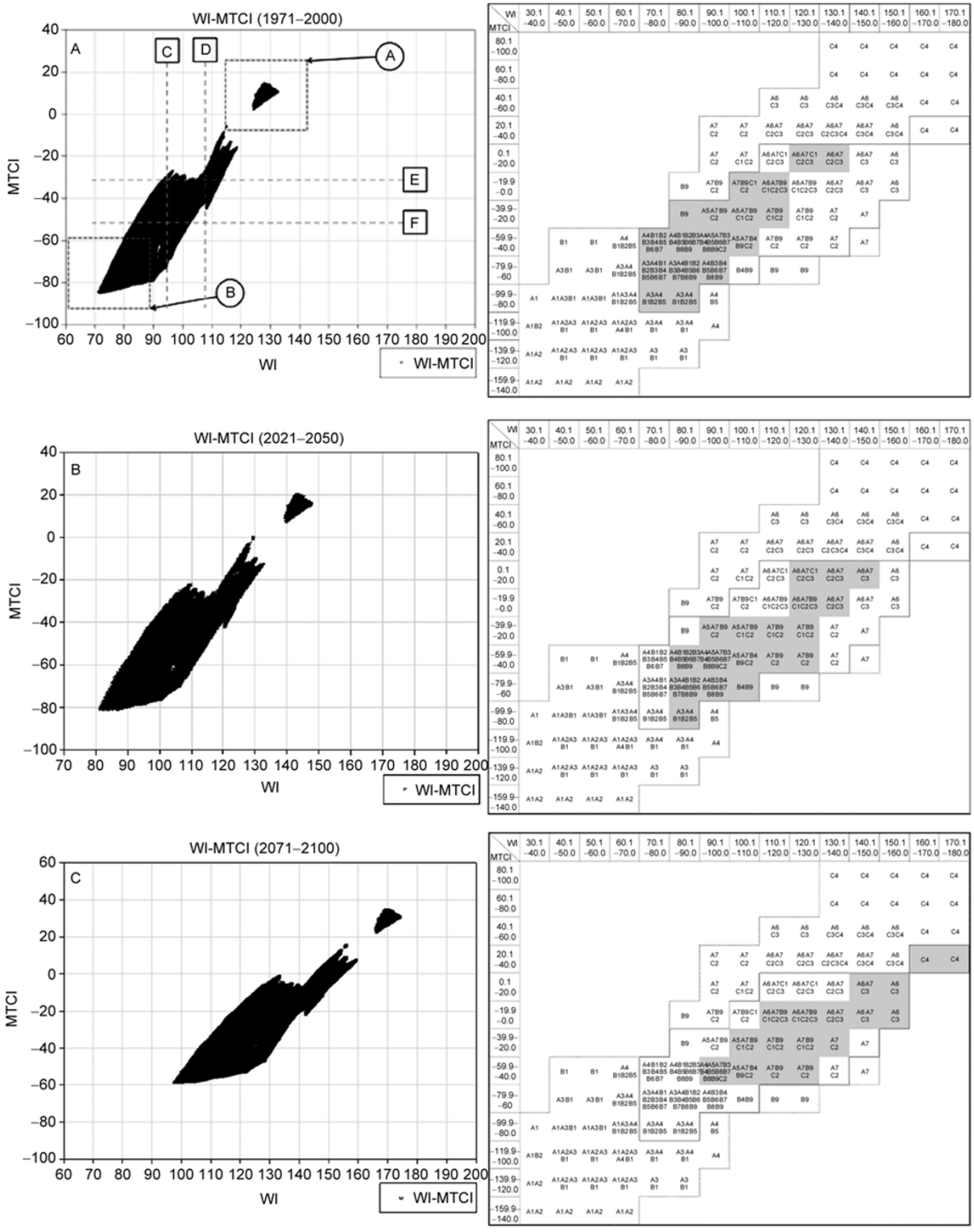

Figure 5 The orthogonal integration changes of WI and MTCI with tree species composition from the past (1971–2000) (A), near future (2021–2050) (C), and far future (2071–2100) in Korea (C).

both the WI and MTCI will be subject to increase, and the higher WI and MTCI zones, formerly exclusive to south-western Korea, will likely expand towards the northeast due to climate change. In particular, the optimal habitat ranges of the WI and MTCI for *P. densiflora*, *P. koraiensis*, and *Quercus* spp. (Table 1) are likely to be confined to the

northeastern inland areas in the far future (2071–2100).

2.2 Distribution of orthogonal integration of WI and MTCI in Korea

The regional characteristics of the thermal indices are shown in the orthogonally plotted maps of the WI and MTCI (Figure 5). The thermal patterns for Jeju Island are depicted in the top right of the integration maps (in the dotted rectangle A in Figure 5A). The average WI and MTCI for this area are 128.9°C·month (std. dev. 2.31) and 9.1 (std. dev. 3.01), respectively. This corresponds to the optimal WI and MTCI ranges of *Cyclobalanopsis glauca*, one of the evergreen broad-leaved trees. Jeju Island is located in the mid latitudes of the north-west Pacific with hot humid summers and cool winters. *C. glauca* is also an important constituent of the modern warm temperate evergreen broad-leaved forests in the coastal lowland of this island [58]. The thermal patterns of the Taebaek and the Sobaek mountain ranges are plotted in the bottom left of the integration map (in dashed rectangle B in Figure 5A). The WI and MTCI ranges correspond to the habitats of *P. densiflora*, *P. koraiensis* and *Quercus.* spp. (Table 1).

In addition, this two-dimensional map can be applied to show the trends of climate change in thermal gradients. As shown in Figure 5, the orthogonal integration of the WI and MTCI distribution will be shifted to the top right corner as climate change progresses. At the same time, the composition of tree species will change along with the distributional shifts of the WI and MTCI in Korea. Hence, the distribution patterns of TAGs will be changed by future climatic conditions (Figure 5).

In previous studies [35,36,40] analyzing vegetation distribution patterns in Korea, only the WI was applied to classify the pixels via vertical zoning using the dotted lines C and D in Figure 5A. On the other hand, applying horizontal classification via the MTCI helps give a more detailed classification. This is because the MTCI is considered as a complementary classifying index in horizontal zoning (in dashed lines E and F of Figure 5A). This is supported by previous studies of Kong [59,60], who suggested the importance of extreme temperatures, such as the mean maximum temperature for August and the mean minimum temperature for January. In addition, Ohsawa [4] and Matsui *et al*. [5,6] have not only used the mean annual temperature, but also the minimum temperature of the coldest month (MTC) to classify the possible habitats of specific tree species, such as *F. crenata*.

2.3 Clustered TAGs of tree species along the thermal gradient indices

To describe the potential forest distribution over South Korea, 22 TAGs were prepared by grouping analogue compositions of tree species (Figure 6). TAG-1 consisted of *P. koraiensis* and *P. densiflora* for evergreen needle-leaved trees, and *Q. mongolica*, *Carpinus laxiflora* and *Q. serrata* for deciduous broad-leaved trees (Table 3). Kong [59] classified the native Korean conifers, *P. koraiensis* and *P. densiflora,* as mountainous types, and reported that their habitats are easily found in and around Mt. Odae, corresponding historically to the TAG-1 region. In addition, TAGs 8, 10, 11, and 13 are related to *P. thunbergii*, one of the coastal types of conifers in Kong's study [59], which are located in the southern coastal area and on Mt. Gyeryong. Another group, TAG-14, has a composition of *P. yunnanensis* for evergreen needle-leaved trees, *Fagus lucida* for deciduous broad-leaved trees, and *Camellia japonica* and *Cyclobalanopsis glauca* for evergreen broad-leaved trees. This is closely related to the latitudinal and altitudinal distribution of subtropical evergreen broad-leaved trees found in a previous study by Koo *et al*. [61]. In their study, *Camellia japonica* and *Cyclobalanopsis glauca* inhabited a southern coastal area corresponding to −9.0°C of MTC (MTCI −63.6). These native Korean species had their distribution limited by a northern boundary for warmth-tolerance. The other TAGs had individual tree species compositions. Therefore, the disposition of TAGs can represent the distributional patterns of forest vegetation in Korea.

Previous studies [23,35,36] applied a grouping and zoning process to show the features of Korean ecosystem distribution. The grouping processes in these studies may be suitable for zoning on a global or continental scale, but are insufficient to explain the detailed distribution of forest vegetation in Korea on a regional scale. For example, the thresholds of Yim [35,36] resulted in the classification of the Korean forest ecosystems into only five major groups (Figure 7). These were the warm-temperate, temperate zone (southern part), temperate zone (middle part), temperate zone (northern part), and arctic zone. In another example, the simulation of a DGVM (MC1 model) had only four major groups explaining the potential vegetation distribution in Korea (Figure 8). These were grass C4 tall, warm mixed forest (deciduous and evergreen broad-leaved trees dominant), warm mixed forest (evergreen needle-leaved trees dominant) and cool mixed forest [23].

In this study 22 TAGs for Korea were defined in terms of the plant functional type. This was in clear contrast to previous models where only four or five vegetation groups were used to explain the vegetation distribution of Korea. This new technique can, therefore, more specifically explain the effects of climate change at a regional-scale than previous global or continental-scale vegetation models. The results presented in Figure 9 and Figure 10 show that the distribution of TAGs will be likely change by the shrinking of TAGs 1, 2, and 3, which correspond to *P. densiflora* and *P. koraiensis*. The distribution ratio of these will likely change from 11.15% (past) to 2.81% (near future). In addition, change will occur in the expansion of TAGs 18, 19, 20, 21 and 22, which are mainly occupied by evergreen broad-

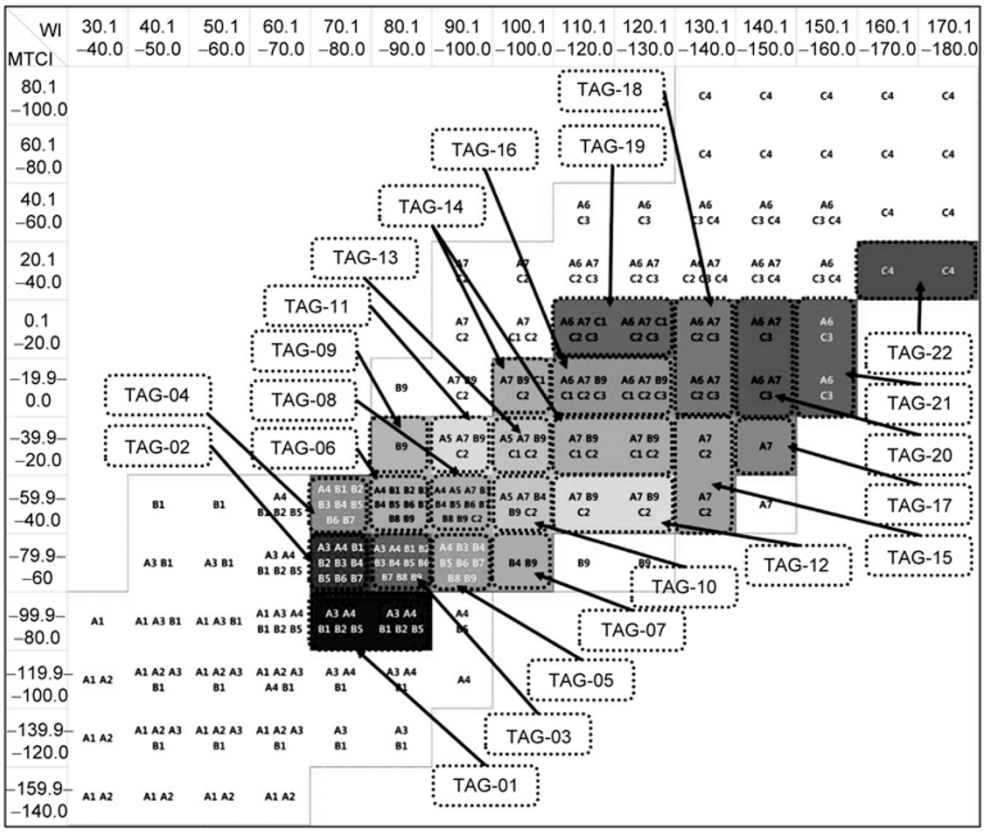

Figure 6 Assigning TAGs based on the analogue composition of tree species.

Table 3 TAGs of tree species along the thermal indices

TAGs	Composition of tree species along the thermal gradients		
	evergreen needle-leaved trees	deciduous broad-leaved trees	evergreen broad-leaved trees
TAG-1	*Pinus koraiensis, *P. densiflora	*Quercus mongolica, *Carpinus laxiflora, *Q. Serrata	
TAG-2	*P. koraiensis, *P. densiflora	*Q. mongolica, *C. laxiflora, *Q. dentata, *C. tschonoskii, *Q. serrata, *Q. aliena, *Q. variabilis	
TAG-3	*P. koraiensis, *P. densiflora	*Q. mongolica, *C. laxiflora, *Q. dentata, *C. tschonoskii, *Q. serrata, *Q. aliena, *Q. variabilis, *Q. acutissima, **Fagus lucida	
TAG-4	*P. densiflora	*Q. mongolica, *C. laxiflora, *Q. dentata, *C. tschonoskii, *Q. serrata, *Q. aliena, *Q. variabilis	
TAG-5	*P. densiflora	*Q. dentata, *C. tschonoskii, *Q. serrata, *Q. aliena, *Q. variabilis, *Q. acutissima, **F. lucida	
TAG-6	*P. densiflora	*Q. mongolica, *C. laxiflora, *Q. dentata, *C. tschonoskii, *Q. serrata, *Q. aliena, *Q. variabilis, *Q. acutissima, **F. lucida	
TAG-7		*C. tschonoskii, **F. lucida	
TAG-8	*P. densiflora, *P. thunbergii, **P. yunnanensis	*Q. dentata, *C. tschonoskii, *Q. serrata, *Q. aliena, *Q. variabilis, *Q. acutissima, **F. lucida	**Cyclobalanopsis glauca
TAG-9		**F. lucida	
TAG-10	*P. thunbergii, **P. yunnanensis	*C. tschonoskii, **F. lucida	**Cyclobalanopsis glauca
TAG-11	*P. thunbergii, **P. yunnanensis	**F. lucida	**Cyclobalanopsis glauca
TAG-12	**P. yunnanensis	**F. lucida	**Cyclobalanopsis glauca
TAG-13	*P. thunbergii, **P. yunnanensis	**F. lucida	**Camellia japonica, **Cyclobalanopsis glauca
TAG-14	**P. yunnanensis	**F. lucida	**Camellia japonica, **Cyclobalanopsis glauca

(*To be continued on the next page*)

(*Continued*)

TAGs	Composition of tree species along the thermal gradients		
	Evergreen Needle-leaved trees	Deciduous Broad-leaved trees	Evergreen Broad-leaved trees
TAG-15	******P. yunnanensis*		******Cyclobalanopsis glauca*
TAG-16	******P. massoniana*, ******P. yunnanensis*	******F. lucida*	******Camellia japonica*, ******Cyclobalanopsis glauca*, ******Schima superba*
TAG-17	******P. yunnanensis*		
TAG-18	******P. massoniana*, ******P. yunnanensis*		******Cyclobalanopsis glauca*, ******Schima superba*
TAG-19	******P. massoniana*, ******P. yunnanensis*		******Camellia japonica*, ******Cyclobalanopsis glauca*, ******Schima superba*
TAG-20	******P. massoniana*, ******P. yunnanensis*		******Schima superba*
TAG-21	******P. massoniana*, ******P. yunnanensis*		******Schima superba*
TAG-22	******P. massoniana*		******Castanopsis indica*

*, From Yim [35,36]; **, from Fang and Yoda [37–39]

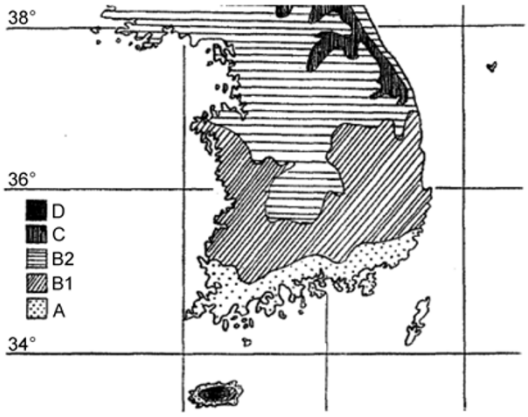

Figure 7 Vegetation distribution plotting results (modified from Yim [35,36]). *A, Warm-temperate, B1: temperate zone (southern part); B2, temperate zone (middle part); C, temperate zone (northern part), and D, arctic zone.

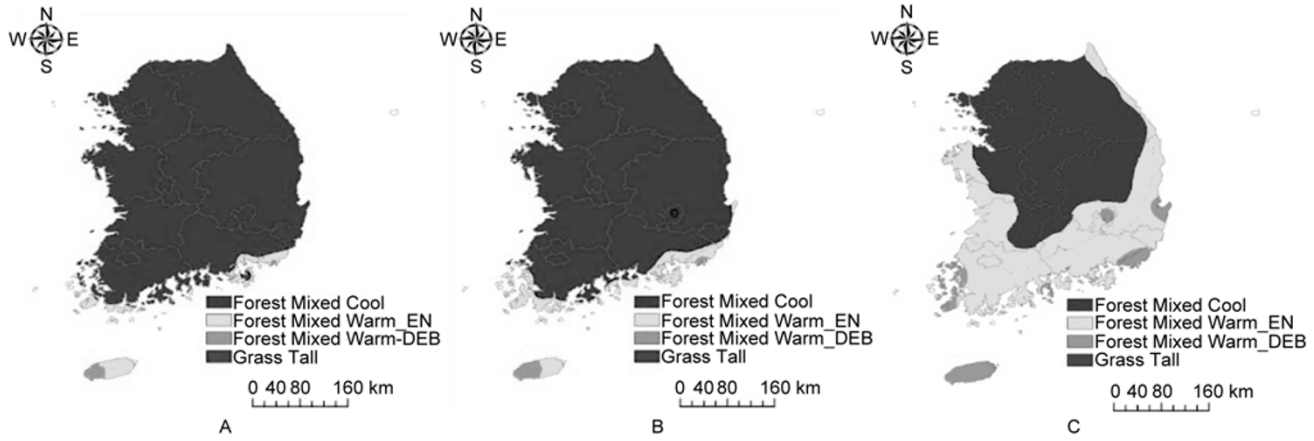

Figure 8 Vegetation distribution simulated by the MC1 model on the past (1971–2000) (A), near future (2021–2050) (B), far future (2071–2100) (C) (Choi *et al*. [23]). *EN, Dominant of evergreen needle-leaved species; DEB, dominant of deciduous or evergreen broad-leaved species.

leaved trees such as *Camellia japonica*, *Cyclobalanopsis glauca*, and *Schima superba*. Here the predicted distribution ratio changes from 1.76% (past) to 1.97% (near future) and 36.44% (far future). As shown in Figure 9A, based on the past climatic conditions (1971–2000), TAGs 1, 2, and 3 cover a relatively high mountainous region in Korea. However, as shown in Figures 9B and C, the area of these TAGs will decrease in the near future (2021–2050), and will be lost from their original habitats in the far future (2071–2100). In the past (1971–2000), TAGs 13 and 14 were well

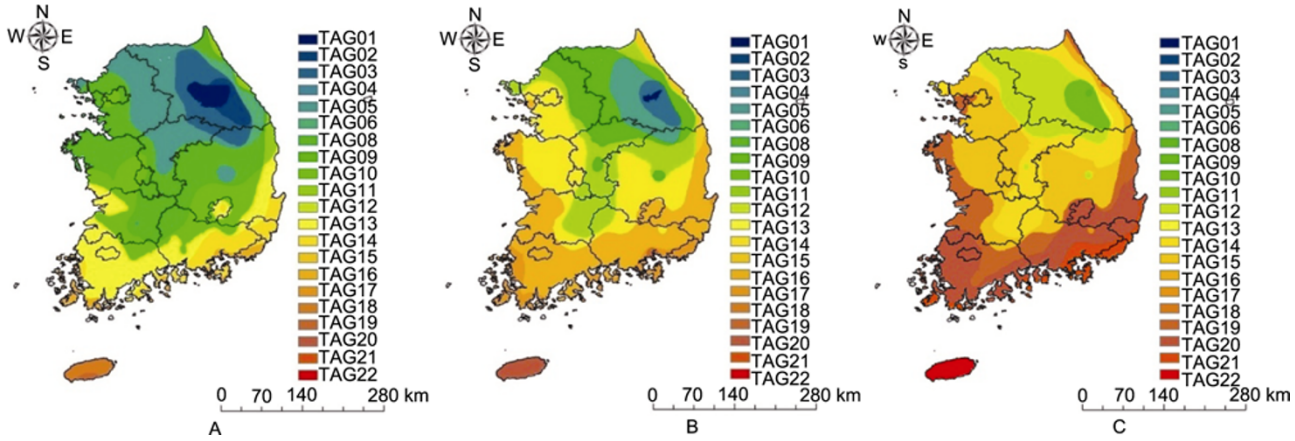

Figure 9 Changes in vegetation distribution of the past (1971–2000) (A), near future (2021–2050) (B), and far future (2071–2100) (C), depicted by the TAGs.

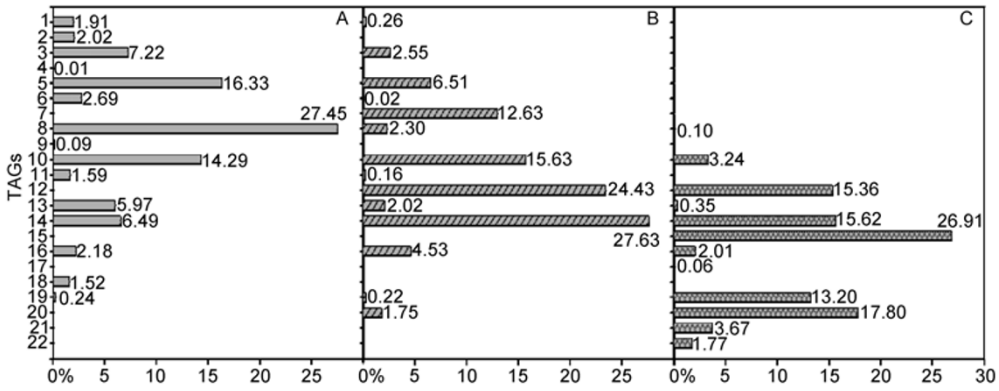

Figure 10 Changes in the TAG distribution ratio of the past (1971–2000) (A), near future (2021–2050) (B), and far future (2071–2100) (C).

distributed in the southern inland and eastern coastal areas. As a result of climate change, these two TAGs gradually lose their past habitats and are predicted to shrink to the eastern mountainous regions (2071–2000). Similar patterns have been reported in previous studies on the vulnerability assessment of forest vegetation due to climate change [20, 62]. Kim and Lee [20] mentioned that, because the maximum migration speed of these forest populations cannot catch up with climate change expansion, increases in thermal indices might cause a reduction in or extinction of native forest species [20,59,62].

2.4 Model verification

As a model verification, we selected specific forest species, such as *P. densiflora* and *P. koraiensis* by merging TAGs 1, 2, 3, 4, 5, 6, and 8. As mentioned in the method, *P. densiflora* is one of the most widely distributed tree species in South Korea (1473000 ha: 23.1% of total forest area). Also, *P. koraiensis* occupies 3.6% (230000 ha) of Korea's total forest area. The total ratio of TAGs related to *P. densiflora* and *P. koraiensis* has been historically 57.63%. After exclusion of the anthropogenically affected area, the total area of TAGs related to *P. densiflora* and *P. koraiensis* was 3714076 ha. This is an overestimation of about 1.54 times, compared to the actual forest distribution. The reason of this overestimation is that the TAGs (1–6, and 8) also include other tree species, such as *Quercus.* spp and *Cyclobalanopsis glauca*. Therefore, the rank weighed system (e.g. Iverson and Prasad [56]) was required to consider the tree species composition in each TAG. We assumed a weighted rank based on a scope of the optimal habitat WI for each species [63] (Table 4). In addition, we compared the TAG results with the 4th actual forest type map of the Korean Forest Service, and estimated the area of A_{both} identified in both TAG results and the 4th forest type map of KFS.

As results of the model verification, the areas of A_{both}, A_{act}, and TA_{pred} were 761791, 711209, and 626979 ha, respectively. The CA equation (Equation 5) revealed a measure of 56.93% accuracy of TAGs to simulate vegetation distribution (Figure 11 and Table 5).

3 Conclusions

The main objective of this study was to predict the effect of

Table 4 Rank weighted system for TAGs (1–6, and 8) and area for each species

Species code		A3	A4	A5	A7	B1	B2	B3	B4	B5	B6	B7	B8	B9	C1
Optimal WI range (°C · month)		45.0–81.0	60.0–95.0	93.0–104.0	90.5–147.1	46.0–90.0	67.0–94.0	75.0–97.0	77.0–103.0	67.0–92.0	75.0–91.0	77.0–95.0	85.0–99.0	87.3–120.9	97.6–137.4
Scope (°C · month)		36	35	11	56.6	44	27	22	26	25	16	18	14	33.6	39.8
TAG	*R	**Area for each species based on the rank weight and distribution ratio (thousand ha)													
01	1.91	27	26			32	20			18					
02	2.02	19	18			23	14	12	14	13	8	9			
03	7.22	56	55			69	42	35	41	39	25	28	22	53	
04	0.01		106			133	82	67	79	76	48	54			
05	16.33		194					122	144	139	89	100	78	187	
06	2.69		23			29	18	15	17	17	11	12	9	22	
08	27.45		208	66	337			131	155	149	95	107	83	200	237
Total	57.63	102	525	66	337	154	94	314	371	375	228	257	192	462	237

*, R: Distribution ratio of TAGs in the past year (1971–2000); **, total area of TAGs is 3714076 ha.

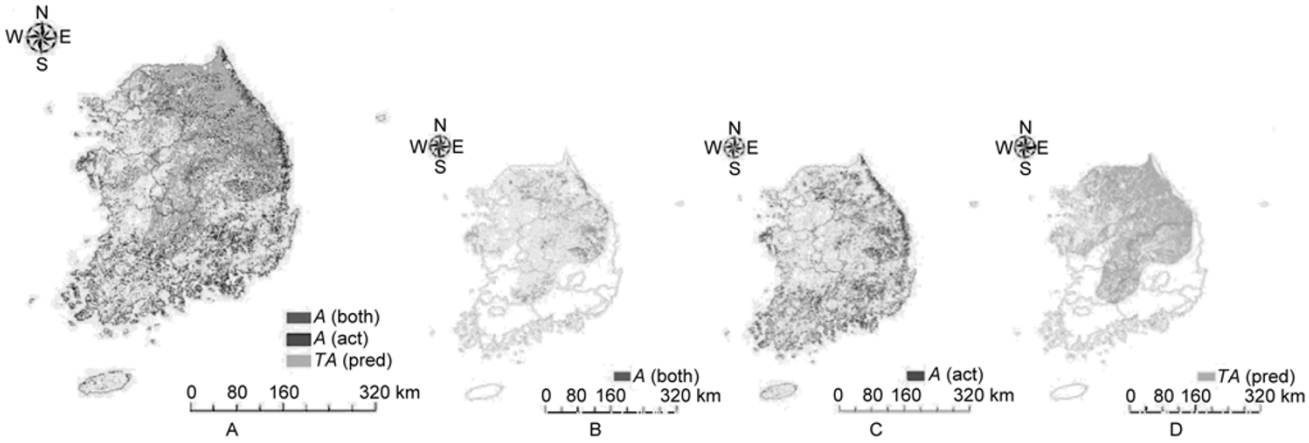

Figure 11 Distribution of A_{both} (in both TAG and forest type map) (A), A_{act} (in forest type map) (B), and TA_{pred} (in TAG simulation) (C).

Table 5 TAG verification

Criteria	Area (ha)
A_{both}	761791
A_{act}	711209
TA_{pred}	626979
Classification accuracy (CA)	56.93%

climate change on vegetation distribution in South Korea. Orthogonal integration of Kira's Warmth Index (WI) and the Minimum Temperature of the Coldest Month Index (MTCI) were plotted to classify the distribution patterns of tree species. Based on the optimal thermal ranges of tree species, the Thermal Analogy Groups (TAGs) in the analogue composition of tree species were designated to explain the vegetation distribution in Korea. This attempt allowed the relatively specific patterns of vegetation distribution change due to climate change in Korea to be explained in greater detail than in previous investigations. Firstly, the results of this study showed that the 22 TAGs correspond to geographical characteristics and ecological features of Korea. Secondly, we were able to predict the influence of climate change as a shrinkage of areas for TAGs 1, 2, and 3, corresponding to *P. densiflora* and *P. koraiensis,* and the expansion of range areas for TAGs 18, 19, 20, 21, and 22, mainly occupied by *Camellia japonica*, *Cyclobalanopsis glauca*, and *Schima superba*.

However, CA verification indicated that the validation value of the TAG model was only 56.93%. In addition, this TAGs model can only predict potential vegetation distribution corresponding to thermal indices. For a more reliable prediction of ecosystem change, it is important to also consider current distribution conditions and human-related impacts. Satellite-based information may be valuable in such fuller diagnostic models where current environmental features and human activities for ecosystem areas can then be considered. In contrast the current prognostic model uses only climatic information to explain the ecosystem. In addition this study predicted only distributional changes of vegetation, but it was not able to assess the carbon fluxes in ecosystems. To achieve this it would need to consider not only climatic conditions, but also other environmental and physiological conditions such as soil moisture, soil temperature, initial biomass and competition amongst species. This challenge may be met by tree growth and physiological

forest models. These models can simulate the growth of deciduous and multiple storied tropical forests, and estimate carbon fluxes in forest ecosystems. In further research, coupling of the TAG model and carbon flux models will be conducted to predict the future impact of climate change on vegetation distribution and carbon dynamics in the terrestrial ecosystems of Korea. Also, it can be applied to vulnerability assessment of forest ecosystems to climate change using the assessment criteria include the sensitivity and adaptation capacity of vegetation distribution to climate change.

This work was supported by the Korea Forest Research Institute research project "Impact Assessment of Climate Change on Forest Ecosystem and Development of Adaptation Strategies" (*Grant No. FE 0100-2009-01*) *and by a research grant from the Korea Science and Engineering Foundation* (*Grant No. A307-K001*).

1 IPCC. Contribution of working group I to the fourth assessment report of the intergovernmental panel on climate change. In: Solomon S, Qin D, Manning M, *et al*. eds. Climate Change 2007: the Physical Science Basis. Cambridge, UK: Cambridge University Press, 2007a. 1032
2 IPCC. Contribution of working group II to the fourth assessment report of the intergovernmental panel on climate change. In: Parry M L, Canziani O F, Palutikof J P, *et al*. eds. Climate Change 2007: Impacts, Adaptation and Vulnerability. Cambridge, UK: Cambridge University Press, 2007b. 976
3 Arris L L, Eagleson P S. Evidence of a physiological basis for the boreal-deciduous forest ecotone in North America. Vegetatio, 1989, 82: 55–58
4 Ohsawa M. Latitudinal pattern of mountain vegetation zonation in southern and eastern Asia. J Veg Sci, 1993, 4: 13–18
5 Matsui T, Yagihashi T, Nakaya T, *et al*. Climate controls on distribution of *Fagus crenata* forests in Japan. J Veg Sci, 2004a, 15: 57–66
6 Matsui T, Yagihashi T, Nakaya T. Probability distributions, vulnerability and sensitivity in *Fagus crenata* forests following predicted climate changes in Japan. J Veg Sci, 2004b, 15: 605–614
7 Laurent J M, Bar-Hen A, Francois L, *et al*. Refining vegetation simulation models: From plant functional types to bioclimatic affinity groups of plants. J Veg Sci, 2004, 15: 739–746
8 Horikawa M, Tsuyama I, Matsui T, *et al*. Assessing the potential impacts of climate change on the alpine habitat suitability of Japanese stone pine (*Pinus pumila*). Land Ecol, 2009, 24: 115–128
9 Prentice I C, Cramer W, Harrison S P, *et al*. A global biome model based on plant physiology and dominance, soil properties and climate. J Biogeo, 1992, 19: 117–134
10 Lenihan J M, Neilson R P. A rule-based vegetation formation model for Canada. J Biogeo, 1993, 20: 615–628
11 Brzeziecki B, Kienast F, Wildi O. Modeling potential impacts of climate change on the spatial distribution of zonal forest communities in Switzerland. J Veg Sci, 1995, 6: 257–268
12 Bachelet D, Lenihan J M, Daly C, *et al*. MC1: a dynamic vegetation model for estimating the distribution of vegetation and associated carbon, nutrients, and water. U.S. Department of Agriculture, Forest Service, Pacific Northwest Research Station, Technical documentation, version 1.0, 2001
13 Cao M K, Woodward F I. Dynamic responses of terrestrial ecosystem carbon cycling to global climate change. Nature, 1998, 393: 249–252
14 Osborne C P, Mitchell P L, Sheehy J E, *et al*. Modeling the recent historical impacts of atmospheric CO_2 and climate change on Mediterranean vegetation. Global Change Biol, 2000, 6: 445–458
15 Watanabe T, Yokozawa M, Emori S, *et al*. Developing a multilayered integrated numerical model of surface physics-growing plants interaction (MINoSGI). Global Change Biol, 2004, 10: 963–982
16 Lenihan J M, Drapek R, Bachelet D, *et al*. Climate change effects on vegetation distribution, carbon, and fire in California. Ecol Appli, 2003, 13: 1667–1681
17 Lenihan J M, Bachelet D, Neilson R P, *et al*. Response of vegetation distribution, ecosystem productivity, and fire to climate change scenarios for California. Climatic Change, 2008, 87: S215–S230
18 Yu L, Cao M K, Li K. Climate-induced changes in the vegetation pattern of China in the 21st century. Ecol Res, 2006, 21: 912–919
19 Kim S N, Lee W K, Son Y. Applicability of climate change impact assessment models to Korean forest (in Korean with English Abstract). J Korean For Soc, 2009, 98: 33–48
20 Kim J U, Lee D K. A Study on the vulnerability assessment of forest vegetation using regional climate model. J Korean Environ Res Rev Technol, 2006, 9: 32–40 (in Korean with English Abstract)
21 Lee M A, Lee W K, Son Y. Sensitivity and adaptability of vegetation and soil carbon storage to climate change with CEVSA model in Korea. Proceedings of A3 Foresight Program, Seoul, Korea. 2007a, 24
22 Choi S, Lee W K, Kwak H B. Predicting the vegetation distribution and terrestrial carbon-fluxes using MC1 model. Proceedings of ESRI International User Conference 2009, San-Diego, USA, 2009a. [2009-07-14]. http://proceedings.esri.com/dvd/uc/2009/uc/abstracts/a1479.html
23 Choi S, Lee W K. Simulating Vegetation Responses and Carbon Fluxes to Climate Change using MC1 Model, Proceeding of IUFRO Conference–International Conference on Multipurpose Forest Management–Strategies for Sustainability in a Climate Change Era. Niigata, Japan, 2009b, 40
24 Riera J L, Magnuson J J, Vande Castle J R, *et al*. Analysis of large-scale spatial heterogeneity in vegetation indices among North American Landscapes. Ecosystems, 1998, 1: 268–282
25 Mather J R, Yoshioka G A. The role of climate in the distribution of vegetation, An assoc amer geog, 1968, 58: 29–41
26 Woodward F I. Climate and Plant Distribution–Chapter 5: Climate and the Distribution of Taxa. Cambridge: Cambridge University Press, 1987. 117–160
27 Woodward F I, Lomas M R, Kelly C K. Global climate and the distribution of plant biomes. Philos Trans R Soc London [Biol], 2004, 359: 1465–1476
28 Looman J. Distribution of plant species and vegetation types in relation to climate. Vegetation, 1983, 54: 17–25
29 Zhang X, Friedl M A, Schaaf C B, *et al*. Climate controls on vegetation phonological patterns in northern mid- and high latitudes inferred from MODIS data. Glob Change Biol, 2004, 10: 1133–1145
30 Jolly W M, Nemani R, Running S W. A generalized, bioclimatic index to predict foliar phenology in response to climate. Glob Change Biol, 2005, 11: 619–632
31 Wang Z H, Brown J H, Tang Z, *et al*. Temperature dependence, spatial scale, and tree species diversity in eastern Asia and North America. Proc Natl Acad Sci USA, 2009, 106: 13388–13392
32 Kim J J, Hong S G, Yoon J K. Effect of minimum night temperature on growth of seedlings of *Pinus densiflora* and *Betula platyphylla* in container culture during winter season. J Bio-Environ Control, 2002, 11: 163–167
33 Sakai A. Freezing tolerance of evergreen and deciduous broad-leaved trees in Japan with reference to tree regions. Low Temp Sci-Ser B: Biol Sci, 1978, 36: 1–19
34 Sakai A, Paton D M, Wardle P. Freezing resistance of temperate and sub-arctic conifers native to the southern hemisphere. Low Temp Sci-Ser B: Biol Sci, 1979, 37: 107–111
35 Yim Y J. Distribution of forest vegetation and climate in the Korean peninsula III. Distribution of tree species along the thermal gradient. Jpn J Ecol, 1977a, 27: 177–189
36 Yim Y J. Distribution of forest vegetation and climate in the Korean peninsula IV. Distribution of tree species along the thermal gradient. Jpn J Ecol, 1977b, 27: 269–278
37 Fang J Y, Yoda K. Climate and vegetation in China (II) Distribution of main vegetation types and thermal climate. Ecol Res, 1989, 4: 71–83

38 Fang J Y, Yoda K. Climate and vegetation in China (III) Distribution of main vegetation types and thermal climate. Ecol Res, 1990a, 5: 9–23
39 Fang J Y, Yoda K. Climate and vegetation in China (IV) Distribution of main vegetation types and thermal climate. Ecol Res, 1990b, 5: 291–302
40 Yang K C, Shim J K. Distribution of major plant communities based on the climatic conditions and topographic features in South Korea (in Korean with English Abstract). Korean J Environ Biol, 2007, 25: 168–177
41 Strimbeck G R, Kjellsen T D, Schaberg P G, *et al*. Cold in the common garden: comparative low-temperature tolerance of boreal and temperate conifer foliage. Trees, 2007, 21: 557–567
42 National Geographic Information Institute. The National Atlas of Korea 2007, [2007-12-01] http://atlas.ngii.go.kr/english/explanation/natural_1_1.jsp
43 Korea Forest Service. Statistical yearbook of forestry, 2008. Korea Forest Service, Seoul, 2009, Chapter II, 30–32
44 Lee C S, Lee W K, Yoon J H, *et al*. Distribution pattern of *Pinus densiflora* and *Quercus* spp. stand in Korea using spatial statistics and GIS. J Korea For Soc, 2006, 95: 663–671
45 Lee M A, Lee W K, Song C C. Spatio-temporal change prediction and variability of temperature and precipitation (in Korean with English Abstract). J GIS Assoc Korea, 2007b, 15: 1–12
46 Min S K, Legutke S, Hense A, *et al*. East Asian climate change in the 21st century as simulated by the coupled climate model ECHO-G under IPCC SRES scenarios. J Meteor Soc Japan, 2006, 82: 1187–1211
47 Cha Y M, Lee H S, Moon J Y. Future climate projection over East Asia using ECHO-G/S (in Korean with English Abstract). Atmosphere, 2007, 17: 55–68
48 Kira T. A new classification of climate in eastern Asia as the basis for agricultural geography. Horticultural Institute. Kyoto Univ, Kyoto, 1945
49 Neilson R P. A model for predicting continental-scale vegetation distribution and water balance. Ecol Appl, 1995, 5: 362–385
50 Largerloef G S. Empirical orthogonal function analysis of advanced very high resolution radiometer surface temperature patterns in Santa Barbara Channel. J Geophys Res, 1988, 93: 6863–6873
51 Weare B C, Nasstrom J S. Examples of extended empirical orthogonal function analysis. Mon Weather Rev, 1982, 110: 481–485
52 Sparnocchia S, Pinardi N, Demirov E. Multivariate empirical orthogonal function analysis of the upper thermocline structure of the Mediterranean Sea from observations and model simulations. Ann Geophys, 2003, 21: 167–187
53 Tadesse T, Wardlow B D, Ryu J H. Identifying time-lag relationships between vegetation condition and climate to produce vegetation outlook maps and monitor drought. Proceedings of the 22nd Conference on Hydrology-Session 6: Drought Assessment and Prediction, Part II, 2008. [2008-01-22]. http://ams.confex.com/ams/88Annual/techprogram/paper_129370.htm
54 Timmermann A. Detecting the nonstationary response of ENSO to greenhouse warming. J Atmos Sci, 1999, 56: 2313–2325
55 Jensen J R. Introductory Digital Image Processing–A Remote Sensing Perspective, 3rd edition, Chapter 8: Image Enhancement. New Jersey: Pearson Prentice Hall, 2004. 255–256
56 Iverson L R, Prasad A M. Predicting abundance of 80 tree species following climate change in the eastern United States. Ecol Monogr, 1998, 68: 465–485
57 Takyu M, Kubota Y, Aiba S, *et al*. Patterns of changes in species diversity, structure and dynamics of forest ecosystems along latitudinal gradients in East Asia. Ecol Res, 2005, 20: 287–296
58 Chung C H. Vegetation response to climate change on Jeju Island, South Korea, during the last deglaciation based pollen record. Geosci J, 2007, 11: 147–155
59 Kong W S. Selection of vulnerable indicator plants by global warming. Asia-Pacific J Atmos Sci, 2005, 41(2-1): 263–273
60 Kong W S. Species composition and distribution of Native Korean Conifers. J Korean Geog Soc, 2004, 39: 528–543
61 Koo K A, Kong W S, Kim C K. Distribution of evergreen broad-leaved plants and climatic factors. J Korean Geog Soc, 2001, 36: 247–257
62 Lee D K, Kim J U. Vulnerability assessment of sub-alpine vegetations by climate change in Korea (in Korean with English Abstract). J Korean Environ Restor Reveg Tech, 2007, 10: 110–119
63 Center for Global Environmental Research. The potential effects of climate change in Japan–Chapter 3. In: Nishioka S, Harasawa H, Hashimoto H, *et al*., eds. Climate Changes and Forests. CGER with assistance of the Environment Agency of Japan, Tsukuba, Japan, 1993. 37–44